

# Intergroup violence in bursts or fizzles

Jeroen Bruggeman\*, Don Weenink, Bram Mak

## Abstract

During intergroup confrontations, agitating stimuli such as opponents' threats and provocations can trigger collective violence, even when the usual mechanisms of cooperation, such as norms with sanctions, are absent. We examine video recordings of street fights between groups of young men. Collective violence in their attacks sometimes breaks out in a burst, while at other times it reaches only a fizzle in which only a few group members participate. An adapted Ising spin-glass model demonstrates that these two temporal unfoldings can be predicted by the proportion of unconditional defectors in a focal group.

## 1 Introduction

When observing the unfolding of intergroup violence committed by non-professionals, one notices a burst or a fizzle in the majority of cases. Before punches are thrown, individuals in the focal group and their opponents insult and threaten, and thereby agitate, one another. For this to result in violence by focal group members, they have to be in close proximity and have to have face-to-face contact [15, 14, 36]. When agitation passes a critical level (for example, when one individual is pushed by an opponent), violence can break out in a burst wherein a majority of individuals (or a subgroup from a larger and more dispersed group) participates. Alternatively, the confrontation can fizzle out, even if group members are agitated. In the case of fizzling, one or few individuals push or punch asynchronously, but there is no burst of violence. Additionally, understanding how collective violence unfolds is complicated by other people present on the scene, who may form an audience or try to de-escalate [32, 46, 63]. De-escalation happens often in street fights [47]. Given a common prelude of proximity and agitation mixed with de-escalation, our question is how to explain bursts and fizzles. To this end

---

\*Corresponding author: Jeroen Bruggeman, [j.p.bruggeman@uva.nl](mailto:j.p.bruggeman@uva.nl)

we use the centennial Ising spin-glass model from physics [55, 44], which resulted in a Nobel Prize for Parisi (2021), and has been used occasionally in the social sciences in various studies of social influence [12, 54, 29, 22]. We apply the model to videos of street fights between groups of (mostly) young men.

Collective violence involves a dilemma of collective action [26, 43, 42], so before predicting bursts and fizzles, we must first address how the Ising model explains overcoming such dilemmas. The face-to-face contacts of the focal group members are the social ties of their network. We already know from public goods experiments that more than half of the participants are conditional cooperators willing to contribute if others do [13], thus conforming to their (weighted) average neighbor in the network [7, 57]. Our empirical study is about relatively inexperienced individuals, rather than seasoned fighters, hence our subjects experience uncertainty when they come under threat, which increases the likelihood of their conforming to the group [65, 39]. Conformity makes sense from an evolutionary perspective when payoffs are hard to predict [59]. Therefore subjects' intentionality not only depends on their expected payoff (as a share of the public good, in this case attack of or defense against opponents) but also their desire to align with their group members.

Now think of two individuals, each with the behavioral options to defect or cooperate. (Behavioral options correspond to magnetic spins in the original model, but that does not matter here.) The possibilities are: (1) both individuals defect, which avoids exploitation but does not yield any public good; (2) one individual freerides the cooperating other, yielding half of the public good; or (3) both cooperate at a cost, which maximizes the public good. The dashed line in Fig. 1 plots these possibilities, with the normalized number of cooperators ( $N_C/n$ ) from left to right. At the beginning, both defect (the local minimum of  $H$  on the left). The vertical axis ( $H$ , or energy in the original) conveys that moving uphill (i.e., that one of the two will start contributing to the public good) is unlikely. By contrast, if moving to lower levels of  $H$  is possible, it will certainly happen; thus, if one of the two cooperates, the other conditional cooperator will join in, and the curve goes to the global minimum of  $H$ , on the right. The hill is the graphical representation of the dilemma of collective action; it is also drawn for a group of five. It shows that without a driving force, it is very unlikely that a group of non-fighting individuals ( $n \geq 2$ ) will overcome the hill and fight collectively, and it is even less likely in larger groups.

Nonetheless, some individuals may start fighting, which in turn may prompt others to join. When agitating stimuli, such as opponents' threats, increase, one or few individuals may accidentally cooperate. This phenomenon of accidental, or spontaneous, cooperation—called “trembling hands” in game

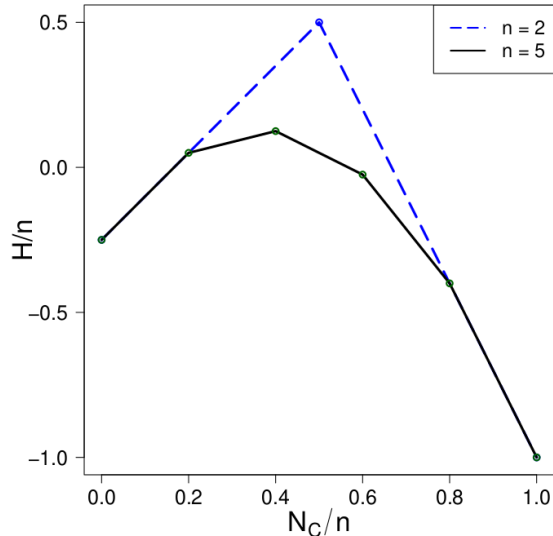


Figure 1: The dilemma of collective action presented as a hill between full defection (left) and full cooperation (right), with the proportion of cooperators ( $N_C/n$ ) on the horizontal axis. The vertical axis ( $H/n$ ) could be intuited as a negative likelihood; moving uphill from a state of defection ( $N_C/n = 0$ ) is very unlikely. One line (dashed) is drawn for a dyad and one for a clique of five individuals. The larger the group is, the more rounded the hill becomes.

theory [17]—can influence proximate others and may result in a cascade of cooperation. For the model, we define turmoil ( $T$ , or temperature in the original) as opponents’ behavior that agitates members of the focal group. If turmoil increases beyond a critical level ( $T_c$ ), fighting can break out in a burst.<sup>1</sup> Our contribution is to show that the outbreak of collective violence depends on a second critical level, namely the critical proportion of unconditional defectors in the focal group ( $p_c$ ). In violent situations, people may defect for several reasons. They may be too scared to fight [15], have empathy with their opponents, disagree with violence (i.e., appraise the public good differently), try to de-escalate, be stopped in their tracks by de-escalators (or guardians), or they may have fought but were wounded, were wrestled to the ground, or became exhausted at some point and became passive. If, for whatever reason, their proportion stays below the critical level ( $p \leq p_c$ ), turmoil ( $T \geq T_c$ ) will be followed by a burst of violence, but above the crit-

<sup>1</sup>The interesting question of why some people self-select into groups where they can fight against others is beyond the scope of this study.

ical level ( $p > p_c$ ), there is neither a critical level of turmoil nor a burst, and violence occurs in a fizzle. The critical level of steady defectors does not follow from earlier theories, but the Ising model allows us to infer it, which we use as a prediction that we test empirically. Note that  $p$  incorporates not only de-escalators in the focal group, but also focal group members who have been prevented from fighting by de-escalators in the focal group or by others.

Most models in the literature revolve around individual rewards and punishments, called selective incentives [42], on top of a share of the public good. These incentives require norms about (in)appropriate behavior in a given situation [19], as well as monitoring of group members [48], and transmission of information (i.e., gossip) through the group's network, which leads to reputations [41] that feed back through selective incentives, with or without leaders. This package of mechanisms is crucial for ongoing cooperation in the longer run but needs time to develop, which may not be available when threats are imminent. The more time people have, the better they can prepare themselves, which is especially important for high-risk situations. Examples of well-prepared groups are police, soldiers, firefighters, and combat medics who receive professional training that enables them to cooperate effectively and respond to situational stimuli in predetermined manners rather than spontaneously. By contrast, ordinary citizens who face violent opponents are far less prepared, or not prepared at all. For unprepared groups, the uncertainties (of outcomes, benefits, and costs) are higher.

Some earlier models of cooperation do not feature the usual package of cooperation mechanisms; namely, models of thresholds [25], cascades [61], and critical mass [35]. They draw on people who take the initiative or leaders to set cooperation in motion. They also draw on strong rationality assumptions, such as perfect information on the numbers of cooperators. It has been found that in protests, however, leaders often proscribe violence, and most violence occurs in the absence of leaders [27]. Hence, the presence of leaders rarely explains the outbreak of violence. The Ising model, in contrast, points out how cooperation can start spontaneously without leaders, galvanized by accidental cooperators rather than exceptionally zealous ones.<sup>2</sup> If there are initiative takers or leaders [23], however, they can be accommodated, and people may also enter and leave a focal group. The Ising model is also more parsimonious than the aforementioned models because it does not rely on assumptions of strong rationality; the degree of rationality is bounded in violent and other uncertain situations due to incomplete information about opponents and group members beyond face-to-face contact.

---

<sup>2</sup>This was already known for the prisoners' dilemma [17].

## 2 Model

Members of a (fledgling) focal group, indexed  $i$  or  $j$ , can defect,  $D$ , or contribute,  $C$ , to a public good, with  $0 < D < C$ . Behavioral variable  $S_i$  of conditional cooperators can take the value  $S_i = C$  or  $S_i = -D$ , whereas unconditional defectors stay put at  $S_j = -D$ . Before a collective action, everyone in a focal group defects. Network ties among focal group members,  $A_{ij} > 0$ , mean that  $i$  is in close proximity to, and senses the behavior of, group member  $j$ , or else  $A_{ij} = 0$ . Because people tend to respond to proportions of their social environment rather than absolute numbers [61, 21], ties are row-normalized, with  $w_{ij} = A_{ij}/\sum_{j=1}^n A_{ij}$  such that  $\sum_{j=1}^n w_{ij} = 1$ . We assume that sensing is reciprocal to at least some degree but not necessarily symmetrical, and that in our small groups ( $n < 10$ ), everyone senses all others, thus the network is fully connected.<sup>3</sup> Opponents' turmoil, represented by  $T$ , has an effect on the focal group at the aggregate level and affects everyone equally. Locally varying turmoil is discussed elsewhere [9]. The Ising model is the following Hamiltonian equation [5, 60]

$$H = - \sum_{i \neq j}^n w_{ij} S_i S_j. \quad (1)$$

We do not assume that individuals know their payoffs in advance, but they will heuristically—and perhaps wrongly—distinguish between valuable ( $C > D$ ) and nonvaluable ( $C < D$ ) public goods or, to the same effect, between potentially efficacious and non-efficacious actions [49]. Note that payoffs are not used in the model's calculations but are defined to provide a meaningful interpretation. When  $i$  chooses between  $C$  and  $D$  amid  $N_C$  cooperators, payoffs for cooperation and defection are, respectively

$$P_C = \theta(N_C + 1)/n - 1 \quad (2)$$

$$P_D = \theta N_C/n + Q \quad (3)$$

with a synergy or enhancement factor  $\theta \geq 1$ . These definitions are the same as in evolutionary game theory [45] except for  $Q$ . This additional factor  $Q$  assures that if  $D$  approximates  $C$ , which means that the outcomes of defection and cooperation become equally valuable,  $P_D$  approximates  $P_C$ .<sup>4</sup>

For our empirical study, we have to choose values for  $C$  and  $D$  to predict the critical level of unconditional defectors,  $p_c$ . The most obvious choice is

---

<sup>3</sup>Temporary exceptions to full connectedness were groups where some people's view was blocked by objects, opponents, or bystanders, as well as one larger group ( $n = 14$ ). These cases we investigated through simulations.

<sup>4</sup> $Q = (\theta/n - 1)(1 - R)$ ;  $R = (C - D)/(C + D)$ ;  $\theta = \theta_0 + R$ , with a base rate  $\theta_0 \geq 1$ .

$C = 1$ , as in game theory and the original Ising model. For  $D$  we want to avoid two trivial values: if  $D = 1$ , there is no point in cooperating, and if  $D = 0$ , there is no dilemma (but a downward slope to the right in Fig. 1). Choosing  $D$  to be maximally distant from the trivial values seems to be a reasonable first approximation, hence we set  $S = \{1, -1/2\}$  for all conditional cooperators, also in the examples. Because these two values were published earlier [10], one could say they were preregistered. For unconditional defectors we set  $S_j = -1/2$ , irrespective of their reasons. Note that all earlier Ising models had either the values  $\{1, -1\}$  [12, 54, 22, 64] or  $\{1, 0\}$  [16]. Of all these models, only one represents a public goods game, in this case for two individuals [1, 50] whereas our model is applicable to groups of any size.

Beyond our empirical study, the payoffs in the asymmetric Ising model can be generalized by relating  $C$  and  $D$  to the symmetric model through a mapping  $\{C, -D\} \rightarrow \{S_0 + \Delta, S_0 - \Delta\}$ , with a bias  $S_0 = (C - D)/2$  with respect to 0, and the two behavioral options symmetrical at each side of  $S_0$  at an offset  $\Delta = \pm(C + D)/2$ .<sup>5</sup> (One could further generalize to variation across individuals, at the cost of many degrees of freedom.) The bias and offset are expressed in the payoffs through  $R = S_0/\Delta$ . If  $\Delta$  is set to a fixed value (0.75 in our examples), decreasing  $S_0$  makes cooperation less valuable, and is equivalent to an increasing proportion of cooperating network neighbors winning over an actor to cooperate, also in other binary decision models [61, 25]. Increasing  $S_0$  makes cooperation more valuable, and it corresponds to a decreasing proportion of cooperating network neighbors.

Solving the Ising model boils down to minimizing  $H$ , which can be done analytically by a mean field approach (in the Supplementary Material). It abstracts away from the network structure, which is no problem for our fully connected networks, and focuses on the mean behavior. We prove that, if  $C = 1$  and  $D = 1/2$ ,  $p_c = 1/3$ . For inhomogeneous (such as clustered) networks, the mean field approach is inaccurate.  $H$  can also be minimized computationally, which is much simpler, and can take inhomogeneous networks into account. Here, we explain the computational approach (Fig. 2). For a given level of turmoil, a network node  $i$  is randomly picked and  $H$  is calculated. For comparison,  $i$ 's current behavior is flipped, from  $D$  to  $C$  or the other way around, and  $H'$  with the flip is calculated. The flip is accepted and implemented if  $H' < H$  or with a certain chance that increases with  $T$ . In other words, increasing  $T$  increases the amount of randomness (due to situational turmoil) in  $i$ 's decision. A behavioral change of  $i$  affects others in

---

<sup>5</sup>It can be shown that the asymmetry in  $S$  is equivalent to the symmetric model with an external field  $2S_0$  [10].

$i$ 's neighborhood when it is their turn to decide. Consecutive decisions are Monte Carlo steps in the Metropolis algorithm [5] that loops through great many Monte Carlo steps (counted by  $t$  in Fig. 2) in order to allow individuals' interdependent behavior to settle down. This procedure is repeated at increments of  $T$ , in our study with step size 0.01.

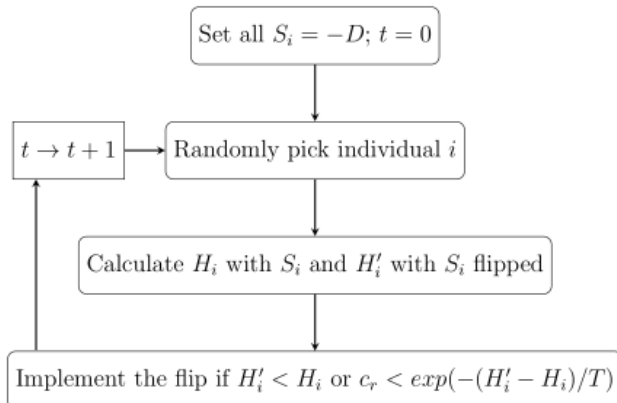


Figure 2: The Metropolis algorithm. Index  $i$  runs over the conditional co-operators (not the unconditional defectors);  $t$  is a counter of Monte Carlo steps;  $c_r$  is a random number in the range  $0 \leq c_r \leq 1$ .

To illustrate the emergence of cooperation with increasing turmoil in a group of  $n = 5$ , we apply the Metropolis algorithm Fig. 3. First, there are only conditional cooperators. At low turmoil, collective action does not start (black line at the top), but at a critical level  $T_c$ , (almost) everybody bursts into cooperation, with a maximum (where  $N_C/n \approx 1$ ) at or near  $T_c$ . Then, a few accidental cooperators win over most others to join the collective action. The effect of turmoil is nonmonotonic and the level of cooperation decreases if  $T$  keeps increasing beyond  $T_c$ , which means that very strong turmoil becomes more confusing than agitating. Fighting ends when exhaustion sets in, a winner stands out (opponents have been wrestled to the ground or have fled), or others intervene.

If there are unconditional defectors,  $T_c$  increases, which is hardly visible in Fig. 3 but more pronounced in larger networks, and maximum cooperation is lower than in the previous case because the number of conditional cooperators is lower.<sup>6</sup> If the proportion of unconditional defectors surpasses a critical level,  $p_c$ , there is a fizzle (dashed blue line in Fig. 3) with much lower levels

<sup>6</sup>In Fig. 1, a proportion of unconditional defectors,  $p$ , means that no matter how many conditional cooperators contribute,  $N_C/n \leq 1 - p$ .

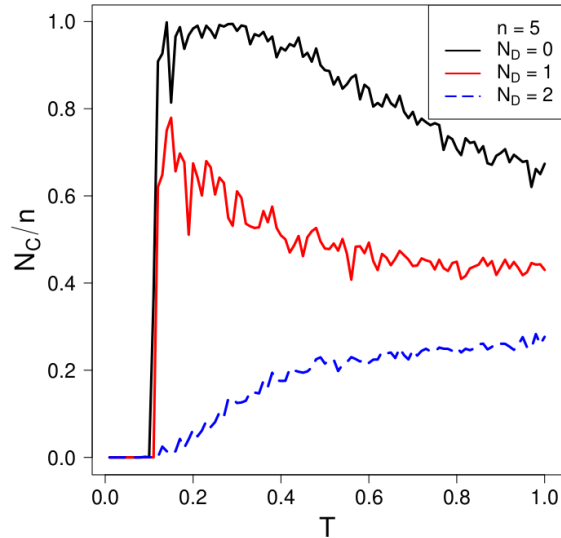


Figure 3: Color online. Proportion of cooperators ( $N_C/n$ ) with turmoil ( $T$ ) in a fully connected network in the size range of our empirical study ( $n = 5$ ); again,  $C = 1$  and  $D = 1/2$ . The black line (top) depicts the group without unconditional defectors ( $p = 0$ ), the red line (middle) a group with one unconditional defector ( $p < p_c$ ), and the dashed blue line (bottom) a group with two unconditional defectors ( $p > p_c$ ).

of cooperation, and no burst-like start of cooperation. In the mean field analysis, there is no (burst of) cooperation if  $p_c > S_0/\Delta$ , independent of network size and density. In simulations,  $p_c$  is proportionally less precise in smaller networks (Fig. 4; Table S3), and the prediction for the triad (red dot in Fig. 4) is empirically false whereas the mean field is correct: one unconditional defector does not prevent cooperation of the other two. Also one empirical group of six with two unconditional defectors had a burst, which is consistent with the mean field but did not happen in the simulations. Based on the mean field analysis ( $p_c = 1/3$ ) and a nearly identical result from the simulations ( $p_c = 0.34$ ),<sup>7</sup> our main prediction is that  $p_c = 1/3$ .

The critical threshold of turmoil increases with network size at a decreasing rate [9], but it also increases with the proportion of unconditional defectors. At  $T_c$ , simulations point out that cooperation starts in small clus-

<sup>7</sup>If unconditional defectors are clustered together in a sparse network, they are less in the way of collective action of the remainder network (thus  $p_c$  is higher) than if they are evenly spread out across the network.

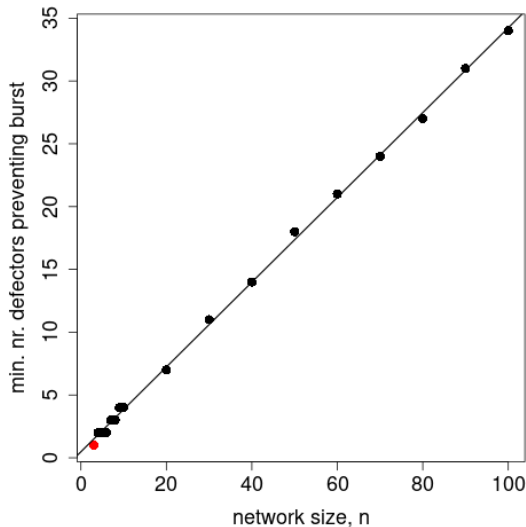


Figure 4: For simulated networks with sizes  $3 \leq n \leq 100$ , the minimum number of unconditional defectors who prevent a burst is plotted. The red dot (left, at the bottom) marks the triad (1 defector prevents a burst of 2), which conflicts with the empirical data (1 defector and a burst of 2).

ters of conditional cooperators, which we will also test empirically.<sup>8</sup> This outcome is puzzling in real life because larger groups have a better chance to win at lower individual costs. Yet if in a small (sub)group, someone starts fighting, he accounts for a relatively large proportion of his neighbors’ social contacts, and more readily wins them over to fight than in a large group where he would comprise a small minority.

### 3 Data and Methods

In studying violence, lab experiments lack the turmoil and emotional intensity of real violent confrontations due to their obligation to meet ethical standards. Field studies, in contrast, cannot be based on a random sample of participants or groups, yet they are invaluable for realistic view on violence [4]. We obtained 42 videos from websites such as YouTube, LiveLeak, and WorldStarHipHop using search terms with the English keywords “brawl,” “street fight,” and “assault.” This sample is random with respect to temporal unfolding and (sub)group size. Of these clips, 36 are from English-speaking

<sup>8</sup>This bottom up mounting of cooperation is similar to bottom up synchronization [3].

countries (mainly the US and the UK, with one from Canada and one from India); five of the remaining clips are from the Netherlands, and one is from Colombia. We did not observe differences in relevant behavior related to the location of the recording. To keep distracting factors away from our analysis, we excluded clips with professional fighters, long range weapons, protective clothing, a referee, ambush attacks, or youths in a school yard. Most of our videos are recorded on phones by bystanders and are left-truncated; in all likelihood, there would have already been some turmoil that motivated bystanders to start filming. The shortest lasted 30 sec. and the longest was nearly 5 minutes (mean 101 sec.; s.d. 59 sec.). Out of a potential 2 x 42 groups, where the opponents in one analysis become the focal group in the next, 25 groups attacked a single individual rather than a group. Because a lone individual is unable to act collectively, this leaves 59 groups to examine; see the Supplementary Material for all case studies and elaborate examples of interpreting and coding. One group had 14 members, but all other groups were small,  $2 \leq n < 10$  (mean 3.6). The smaller groups were simulated as cliques wherein everyone could see one another unless there were obstacles or de-escalators obstructing visual contact.

The videos were coded using Noldus Observer XT 14 software. Clips were played at half speed many times over, and one of us discussed the coding of each with one or two assistants. The assistants were unaware of the theoretical expectations. Each of the 406 individuals was coded for group belonging, and their behavior was interpreted and coded on the timeline.

We coded *violence* when force was used against another's body (punching, slapping, kicking, hitting, stomping) and/or when another person's body was forcefully moved. People may defect (not use violence) for all kinds of reasons and due to various causes. Yet, *unconditional defectors* have in common that they are (temporarily) inactive while others contribute. Among them we include de-escalators, as well as group members who were prevented to fight by de-escalators.

We subsumed the following behaviors of members of the opponent group under *turmoil* for the focal group: aggressing (including fighting gestures); pulling off clothing (jackets or vests); pulling up pants; pointing toward opponents; provocative gesturing with fingers or hands (as an invitation to engage); bending forward toward an opponent; approaching the focal group; encroaching (invading opponents' personal space through using or damaging objects belonging to them); teasing, such as lightly hitting or ridiculing; and violence. Because stumbling and falling because vulnerability of opponents tends to agitate focal group members [15, 40, 62], we included these mishaps in our measure. It is likely that over relatively short time intervals, turmoil accumulates in participants' minds. Therefore we calculated the level of tur-

moil from the beginning of the video until a focal group’s (first) maximum participation in violence. We did this by multiplying the duration of each instance of turmoil by the number of individuals involved, and adding up all these weighted instances. This scale should be improved in future studies, but our main prediction is independent of it.

Given the distraction caused by turmoil, it is not feasible for all group members to react within 1 second to a first cooperater (as they might in a well-organized sports team), whereas 3 seconds is too long for the notion of burst to apply to our small groups. Hence we defined a *burst* as an outbreak of violence by at least half of the group (Fig. 3), or both individuals in a dyad, if they started fighting less than 2 seconds after the first, with a 5% margin.<sup>9</sup>

## 4 Results

Of the 59 groups considered, there were 23 groups where violence started in a burst, 15 groups where violence was collective without a burst, and 21 cases of violence by a single group member. Turmoil preceded all collective violence with one exception, where two individuals suddenly assaulted a passive victim. The critical level of turmoil ( $T_c$ ) for bursts is case-specific and depends on group size, both in absolute number and relative to the size of the opponent group, and on the proportion of unconditional defectors. Additionally, the use of weapons has an intimidating effect.

We confirm the finding of an earlier study [15] that fighting tends to start in small groups or in small subgroups of larger groups. As predicted, we found that small (sub)groups burst into action at lower levels of turmoil than larger groups [9], and lower levels are of course reached earlier. In our data, bursts developed in 13 (37%) of the 35 smallest groups (dyads and triads) and in 10 (42%) of the 24 larger groups. In bursts, the correlation between group size and turmoil is 0.53. The size-turmoil relationship is slightly disturbed by dyads more often facing a larger opponent group and being therefore less likely to fight collectively than triads, which in turn are more robust in general [52]. In fact, larger groups always defeated smaller opponent groups (made them flee or worked them to the ground) with only one exception.

The proportions of unconditional defectors in groups with bursts (mean = 0.19; s.d. = 0.21) and groups without bursts (mean = 0.49; s.d. = 0.27) are box-plotted in Fig. 5 (Welch test  $t = 4.796$ ;  $P = 6.411 \times 10^{-6}$ ;  $df = 54.76$ ). The predicted critical threshold (vertical line in the figure) neatly

---

<sup>9</sup>The requirement that  $N_C \geq 0.5n$  is based on simulations of small networks just above  $p_c$ , but under this condition in large networks (e.g.,  $n = 1000$ ),  $N_C < 0.5n$ .

separates the two boxplots, but one might question how robust this result is, given some noise in coding. There is a risk of missing a violent act (it can be very fast) or mislabeling a fast movement as violence, thus mixing up fighters and defectors, and a risk of misassigning individuals to groups. Even if we suppose there is a 10% chance of each of these errors (which corresponds to Krippendorff’s  $\alpha = 0.75$ ; see inter-coder reliability in the Supplementary Material), the result is hardly weakened (Welch test  $t = 3.879$ ;  $P = 0.0025$ , averaged over 1000 simulation runs), hence the distinction between bursts and fizzles appears to be robust.

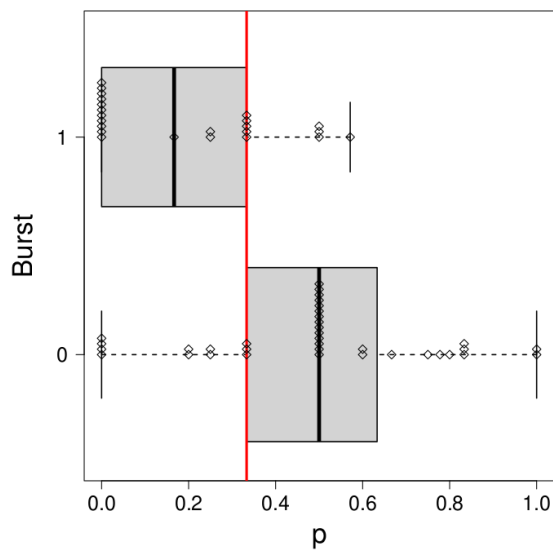


Figure 5: The proportion of unconditional defectors and the predicted critical level (vertical line), which for our data separates the boxplots of bursts (1) and fizzles (0).

The empirical distinction between bursts and fizzles is not perfect, and Fig. 5 shows that 15 groups out of 59 (25%) are categorized incorrectly. In 11 of these 15 groups, the time between the first violent act and last participant joining in was beyond our two-second interval, hence we did not count these collective actions as bursts. In simulations, lags between first instances of violence and the moment when at least half of the group is participating frequently occur when turmoil lingers at its critical level (Fig. 6), versus steadily increasing turmoil that yields a clean burst (Fig. 3). Lingering turmoil seems to have occurred in 4 cases, but we would need a better scale of turmoil than the cumulative scale we currently use to be sure. Far more important are local circumstances beyond the model. When re-examining the

time lags beyond 2 seconds, we noticed various causes of delay: (1) group members were in a car and it took time to get out; (2) a focal group member stood at a distance from the fight on a slippery floor next to a pool; (3) a focal group member was beaten and seemed intoxicated by alcohol, hence responded slowly; (4) a focal group member was first pushed over and it took him time to get on his feet again; (5) opponents moved around so fast that it took time to hit one; (6) an opponent fell into thick bushes such that only one focal group member at a time could get to him; (7) group members were sitting in a train and needed time to get on their feet; (8) group members were constrained in a small room where they searched for a space to lash out; and, (9) group members were hindered by the mess of two opponents fighting on a collapsed table full of food. One can hardly blame the model for not incorporating these local circumstances that caused delays, and perhaps our 2 seconds limit should be applied with more care. Finally, two delays were caused by ambiguous behavior: (10) someone tried to de-escalate, was hit, and then attacked, and (11) someone tried to pull back his fighting friend (de-escalation) but attacked simultaneously.

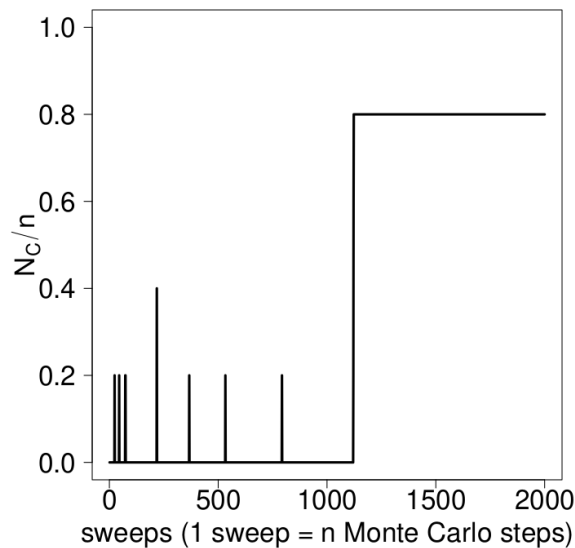


Figure 6: Proportion of cooperators ( $N_C/n$ ) over time (or precisely, over Monte Carlo steps) in a fully connected network ( $n = 5$ ) with one unconditional defector, at  $T = 0.11 \approx T_c$ . Note an extended period of multiple short spikes of violence before all conditional cooperators join in. Similar lags occur without unconditional defectors.

In the 4 out of 15 remaining groups, non-bursts were predicted whereas

bursts occurred. Although for parsimony, we applied the same  $S_0$  (and  $\Delta$ ) for all conditional cooperators, some combatants ( $i$ ) may actually have a higher value than the average,  $S_{0,i} > \overline{S_0}$ , which could explain these cases. In lab experiments, it is unlikely that the patterns of bursts and fizzles would have been discovered, but now they have been pointed out in the field, ethically acceptable intergroup conflicts in the lab may benefit from controlled circumstances, such as equal monetary payoffs for all cooperators, and may lead to refinements of the model.

#### 4.1 Alternative explanation

A plausible alternative explanation for the onset of collective action is synchrony of motion [37], which yields a feeling of oneness among group members [20] and a stronger willingness to take risks for one's group mates [56].

We measured the synchronization of focal group members pairwise if they engaged in the following behaviors simultaneously (i.e., overlapping intervals on the timeline): approaching members of the opponent group at the same pace (normal, energetic, or running), distancing from the opponent group at normal walking speed (we consider simultaneous distancing at energetic or running pace uncontrolled attempts to escape rather than forms of synchrony), or simultaneously engaging in aggressing. To calculate the level of synchrony, we noted the duration of each instance of synchrony from the beginning of the clip prior to the moment of maximum participation in violence, and we multiplied it by the proportion of focal group ties involved (i.e., normalized with respect to the maximum number of ties in the group).

Although in 21 out of 23 bursts, some degree of synchronization (10.8 on average) preceded collective violence, there were 18 cases in which synchronization (9.6 on average) was not followed by collective violence. In some of the latter cases, synchrony turned out to be a deceptive performance composed of blustering and aggrandizing without commitment to fighting. This does not imply that synchronization is unimportant (it probably is for solidarity [15]), but it does not predict collective violence.

## 5 Discussion

The simple Ising model is a century old [31] and has been applied to a wide range of problems [44, 55], to which we add the dilemma of collective action. It explains cooperation parsimoniously, based on agitating stimuli without recourse to strong rationality, initiative takers, reputations, norms, feedback through selective incentives, or reliable information passing through

the network. The Ising model elucidates the temporal unfolding of violence by predicting a critical threshold of unconditional defectors that distinguishes a burst of collective action from a fizzle, which is largely supported by the data. The model also explains why violent groups are often small or are small subgroups of larger groups despite greater risk. Small (sub)groups have a lower critical threshold of turmoil, and in a confrontation with opponents, lower levels are reached earlier. We also investigated whether synchronous action precedes violence, but we found that synchronization precedes both collective and solitary violence, and cannot predict either of these outcomes. However, synchronization may still be important to increase solidarity [18].

This study has several limitations. Because we did not select any videos without violence, we cannot be certain that violence is caused by turmoil. When investigating the videos, however, we observed time and again that people reacted violently to turmoil, hence it still seems quite plausible that turmoil triggers violence. Moreover, the model predicts that when turmoil increases, small groups start cooperating earlier than large groups, which we were unable to falsify. Our measurements underestimated turmoil because the videos are left-truncated, and our data depend on camera angle and vision width, inevitably excluding instances of turmoil. Furthermore, there might be some error in our coding. If the truth were perfectly known and the coding corrected accordingly, the two boxplots in Fig. 5 might shift to a small degree, but this would not affect our main result. In the future, a better scale of agitation should be developed. The scale should differentiate between domains (e.g., street violence versus grievances about politics), thus there should be multiple scales, and these should differentiate between effect sizes of different stimuli. For example, the impact of family members being killed will be much larger and last longer than that of a push, which might be quickly forgotten. Some protest movements are known to produce agitation by themselves, which is sometimes indicated by accelerated posting of online messages. Because in these cases, the inter-posting time intervals follow a certain pattern (Moore’s law),  $T_c$  can be accurately predicted, well ahead of large street demonstrations [28]. Another limitation is in the Ising model itself. Despite predicting the threshold of unconditional defectors well, some of the groups ended up in the non-burst category due to local circumstances (ignored by the model) that caused delays beyond our two second limit. Furthermore, the Ising model does not predict the severity of violence. For future studies, it is important to expand the number and diversity of cases, and to develop better software than is currently available to automatically code videos. Finally, when individuals find themselves more often in similar situations, they will learn, which is easier in smaller groups where they have a larger influence on their payoff [11]. Some will change their strategy, and turn

into unconditional defectors [2] who try to exploit other group members and maximize their individual payoff instead of maximizing the group's payoff. For the model, this would require individuals updating their decision rules at subsequent Monte Carlo steps.

Here we applied the Ising model to violence, but it can also be applied to other uncertain situations. Its dynamics are entirely consistent with temporal patterns of protests [24], which break out more often if (rumors say that) a government or its police are weakened [53, 58], analogous to vulnerable individuals in street fights. The model also seems applicable to spontaneous lynchings [6], and bystanders collectively helping victims under uncertainty [47]. In this first empirical application, we showed that it can explain the unfolding of street violence, and in all likelihood, more discoveries lay ahead. Extensions to norms (as external fields) and noise in actors' information about others' behavior have been explored in simulations [8].

Taking a broader perspective, random noise can solve coordination problems, such as collective responses to opponents' threats, by shaking a group loose from its suboptimal (e.g., non-cooperative) state [51], but it can also disturb an optimal state. In the Ising model, both can happen, depending on the amount of turmoil: when in a group, turmoil approaches  $T_c$  from below, random noise in decision making facilitates cooperation, but at high levels, too much noise entails confusion.

## Ethics

The use of videos for research purposes poses distinct ethical challenges, largely due to the nonanonymous content of the videos. However, ethical guidelines for digital spaces tend to be less restrictive [38], with the consent of the participants being less stringent for data acquired from the public domain, including the internet. While our video corpus is open for use and inspection by other researchers upon request, we require that they take the same measures to ensure the anonymity of the persons portrayed as we did.

## Data availability statement

All coded video data, the R script used to produce plots (Supplementary Material) from the data, and a Fortran script for simulations of the Ising model are available at <https://osf.io/f25nq/>

## —Supplementary Material—

### 6 Data and compilation of data set

In contrast to prior studies of violence and deescalatory action based on CCTV footage [32, 33, 47] most of our videos were captured on mobile phones, which tend to provide better picture clarity, detail and sound. Whereas CCTV footage is most often shot from an elevated and fixed camera angle, people who record violent incidents on their mobile phones tend to follow the action, thereby allowing us to observe bodily positioning and movements in more detail [34].

One concern about phone-recorded clips is that recorders start filming when the antagonism is already ongoing; our data are thus left-truncated to an unknown degree. We discarded footage that immediately started with physical violence. Another concern is that uploaded videos might be biased toward more spectacular cases. However, our sample shows variety in the forms and severity of violence, ranging from groups who engage in frenzied collective violence to incidents that involve just a few slaps. A third concern is whether the recording influenced the behavior of the assailants. Several videos showed more than one person recording the incident. Earlier work [30] noted that a host of research indicates that people do not change their behavior substantially in the presence of a camera and mainly focus on what they are doing. This is probably even more the case in antagonistic situations, and because young people are used to being filmed by phones. Additionally, when people do pay attention to the camera, which happened in just one of our clips, it is visible in the recording and can be incorporated in the analysis. (In our case, this concerned behavior coded as turmoil.)

We used the following criteria to compile our dataset. First, we only included incidents in which at least one of the antagonistic parties comprised at least two members. Second, we only selected clips in which violence could be observed from the (or a) beginning until the end. Third, we focused on fights that seemed to have occurred spontaneously, excluding prearranged fights on the basis of any of the following criteria: the fighters and bystanders all had approximately the same young age (e.g., school yard fights); the antagonists were wearing protective clothing; or a referee was present. Regarding gender, the overwhelming majority of the incidents were between males, with only 8 cases involving both females and males. We excluded female-only fights because they often seemed being arranged (back yard fights with male referees).

Along these criteria, we obtained 42 videos from websites such as YouTube, LiveLeak, and WorldStarHipHop, using search terms with the English key-

words “brawl,” “street fight,” and “assault.” This sample appears to be random with respect to temporal unfolding and (sub)group size. 36 clips are from English-speaking countries (mainly the US and the UK, with one from Canada and one from India); 5 of the remaining clips are from the Netherlands, and 1 is from Colombia. We did not observe differences in relevant behavior related to the location of the recording.

The shortest clip lasted 30 sec. and the longest nearly 5 minutes (mean 101 sec.; s.d. 59 sec.). Out of a potential  $2 \times 42$  groups, where the opponents in one analysis become the focal group in the next, 25 groups fought with a single individual rather than a group, which leaves  $\mathcal{N}=59$  groups to examine. Most groups were small,  $2 \leq n < 10$  (mean 3.6), but one had 14 members (of which 6 became violent). The smaller ones were simulated as fully connected networks wherein everyone could see one another unless there were obstacles or deescalators obstructing visual contact. Obstruction was simulated by removing  $m$  ties.

## 7 Coding

We used Noldus Observer XT 14 software to code the behaviors of individuals, resulting in start times and durations of behaviors per individual throughout the video clip. The software distinguishes state events of relatively longer duration (e.g., holding a person) from point events that are brief single acts (e.g., a punch). When an act of violence took a more extended duration (e.g., holding or dragging), we coded the entire duration of the act, thus creating a state event. When a series of violent point events appeared less than two seconds after one another, we connected them, thus creating a state event.

To enhance the precision of our coding, we coded observable actions (such as kicking, punching, pointing at opponent) and later lumped them together to generate the main codes: violence, turmoil, and deescalation. We coded the behavior of each actor in multiple rounds, coding only one type of action per round. The video material was played at half speed and repeated many times, which is important because violence proceeds too fast to see what is going on in real time. The first 20 clips were coded by one of the authors and two assistants. We discussed the coding when we disagreed and continued the procedure by multiple coders until agreement was reached. At this point, the remainder of the clips were coded by one (meanwhile) experienced assistant researcher and were later checked by another. The remaining disagreements or mistakes were discussed, and the coding was adjusted accordingly.

To identify whether individuals belonged to a focal, opponent, or third-

party group, we observed whether they remained close (at touching distance) to each other as they moved through space, whether they called each other by their names, whether they touched each other (for instance, by tapping shoulders), or whether they shared a vehicle or other object (for instance, a bag or skateboard). One of the authors and two assistants discussed each case in which we observed one or more of these behaviors to determine whether the actors were part of the same group. To assess the reliability of our coding, we asked three students who were unaware of our theoretical expectations and preliminary results to code group memberships, maximum number of participants involved in violence, and the occurrence of bursts in 37 videos, containing 54 groups and 20 solitary individuals (according to our own coding). Notice that just like biologists observing primates, much experience is required to become an accurate observer, which these students did not have. Krippendorff's alphas for group membership, fighters, and bursts were .87, .68, and .75 respectively. We also calculated whether the distinction between bursts and fizzles in students' coding followed the predicted critical proportion of unconditional defectors. We arrived at the number of unconditional defectors (which the students did not code) by deducing the maximum number of participants in violence from the group size. Out of 49 groups (5 cases missing or coded as individual rather than group, as we did) students identified 29 bursts and 20 fizzles (we required that at least 2 out of 3 students agreed on the observation of a burst to denote it as such). The proportion of defectors was .18 (sd = .03) in bursts and .33 (sd = .04) in fizzles (Welch test 8.3, df 35.6,  $P = .007$ ), with bursts clearly below and fizzles right at our critical threshold.

## 8 Composition of indicators

*Violence.* We coded violence when members of the focal group used force against another's person's body (by punching, slapping, kicking, hitting, stomping) and/or when actors moved or held another person's body forcefully (by pushing, shoving, dragging, wrestling, holding, etc.). To enhance the reliability of our coding, we also coded whether actors used their hands, legs, or other body parts (e.g., elbow, head) and whether weapons were used, including the type of weapon, excluding guns (i.e., knives, sticks, tasers and improvised weapons, such as a skateboard or bottle, etc.). We define collective violence as time intervals wherein two or more members of the focal group used violence simultaneously, either as overlapping state events or, in fewer cases, as simultaneously occurring point events. The maximum participation in collective violence was determined by taking the largest number of

focal group members engaging in violent action, divided by the total number of focal group members.

In the videos, it was not possible to distinguish leaders from initiative takers, but we noticed individuals who started violence on their own. In simulations, a leader/initiative taker  $i$  can be incorporated by a larger, individual  $S_{0,i}$  value; the result is collective action at lower  $T$ .

*Unconditional defectors* do not cooperate when  $T \geq T_c$  or most network neighbors cooperate. First, we labeled as unconditional defectors, the focal group members who took deescalatory action towards others. Their behavior was coded as follows [32]: open-handed gestures in the direction of other individuals; waving arms to stop or dampen in the direction of others; touching or patting; guiding a person away; pulling people apart; and putting one's body in between opponents. Whether deescalators' interventions were effective or not, they were at least temporarily unavailable to participate in violence themselves, and their behavior signaled noncooperation to their fellow group members. Second, we noted group members who were effectively stopped from using violence for at least five seconds by other focal group members, opponents, or third-party members (e.g., bystanders). Third, group members remaining passive when others fought. Fourth, group members unable to participate in violence due to spatial constraints for at least five seconds, for instance, due to cars blocking their way or because they were not close enough to the action. Fifth, group members unable to participate for at least five seconds because they were wounded or had fallen to the ground. We took all five reasons for and causes of defection into account for the proportion of unconditional defectors before and during the first instance of violence by the focal group.

*Turmoil.* We subsumed the following behaviors of members of the opponent group under the heading of turmoil for the focal group. First, we coded approaching when opponents moved closer to focal group members. We also indicated whether actors moved energetically (jumping/skipping) and whether they ran. Second, aggressive behaviors when actors in the opponents' group moved body parts in a way that signaled provocation, hostility and/or a readiness to attack. We used the following modifiers (sub-codes) to specify aggressing behavior: fighting gestures; pulling off clothing (jackets or vests); pulling up pants; pointing at opponents; provocative gesturing with fingers or hands (as an invitation to engage); bending forward (head and/or chest bending toward opponent); encroaching (invading opponents' personal space through using or damaging objects belonging to them); and teasing (invading opponents' body space in a teasing/ridiculing way that does not inflict bodily harm, such as lightly hitting, stroking, or patting the opponent's body). Third, involuntary behavior that increases the vulnerability of

opponents, because it tends to agitate (signaling opportunity) and provoke violence. This concerned stumbling and falling to the ground. Finally, violence committed by members of the opponent group. Because we do not know the psychological impact of the various kinds of turmoil, we could not construct a ratio level scale. Instead, we calculated the total level of turmoil from the beginning of the clip until a focal group’s maximum participation in violence by noting the duration of each instance of turmoil, and multiplying it by the number of opponents involved, i.e., the surface area under the turmoil curve in Fig. S10, S13, and S14.

*Bursts.* We identified bursts when, at the first moment of collective violence, two conditions are fulfilled: (1) at least half of the focal group members joined the fight, or both actors did in a dyad, and (2) cooperators started fighting in less than 2 seconds (with a 5% margin) after the first. Condition (1) follows from simulations of small groups; see Table S3. Note that in simulations of much larger networks ( $n \geq 1000$ ), bursts can occur wherein less than half of a group participates. In some videos, we observed multiple bursts; in these cases, we only considered the first burst to facilitate comparison of cases.

## 9 Examples from videos

Graphs of behavior on the timeline enable to analyze and compare the coded videos. Each graph shows the intervals and their durations of (collective) violence, turmoil, synchrony and deescalation (see Fig. S10, S13, S14).

To illustrate, we discuss how coded video data was turned into a graph for clip 26. Fig. S7-9 feature screenshots of the clip, and Fig. S10 displays the graph. This clip features a confrontation of a dyad (focal group) with a triad (opponents) in a restaurant. Violence started at approximately 14 seconds into the video and quickly became collective until approximately 28 seconds. Four instances of turmoil preceded the violence, starting with one of the members of the opponent group gesturing aggressively and walking around in a jumpy, energetic way. The members of the focal dyad walked synchronously toward and away from the opponent in three shorter and one relatively longer stretch of time. Fig. S7 captures a moment of synchrony; the members of the dyad were making fighting gestures and stood aligned, each stretching out one leg with their feet pointing toward the opponent, and the other leg standing backward. Fig. S8 shows the moment when the dyad’s level of agitation reached a critical level; when one of the focal actors dodged backward, avoiding being hit, his companion was about to deliver a blow to the head of the opponent, which made the latter fall down. Fig. S9 displays

the second member of the opponents' triad (soon joined by the third) rushing into the restaurant toward the focal dyad, near his fallen companion. At this point, both groups were engaged in collective violence. Fig. S8 also shows bystanders (who can be seen sitting at a table in Fig. S7) and employees standing near the counter. At 28 seconds, an employee took deescalatory action for the first time. At that point, the collective violence had stopped already and erupted again for a shorter moment approximately 2 seconds later. The clip ends when two triad members carry their fallen group member outside. By then, the focal dyad had already left the scene.



Figure 7: Still taken from clip 26 at 0:06 seconds.

Fig. S11-S13 provide another illustration. Fig. S13 is the graph of clip 86; it shows three outbreaks of collective violence in a group of five members who faced a single opponent. In the first instance of collective violence (not a burst by our 2 seconds criterion), starting at approximately 60 seconds into the clip and lasting for approximately 30 seconds, four members participated. Three of them immediately followed each other, and the fourth joined after approximately 2 seconds. Prior to the outbreak of violence, the opponent agitated focal group members by walking back and forth and by posturing aggressively. Fig. S11 captures the trigger moment of agitation; i.e., while one member of the focal group was engaged in aggressive posturing and a group member tried to deescalate, the opponent was about to strike another



Figure 8: Still taken from clip 26 at 0:13 seconds.



Figure 9: Still taken from clip 26 at 0:15 seconds.

focal group member. Fig. S12 shows the situation 4 seconds later, when three members of the focal group were attacking.

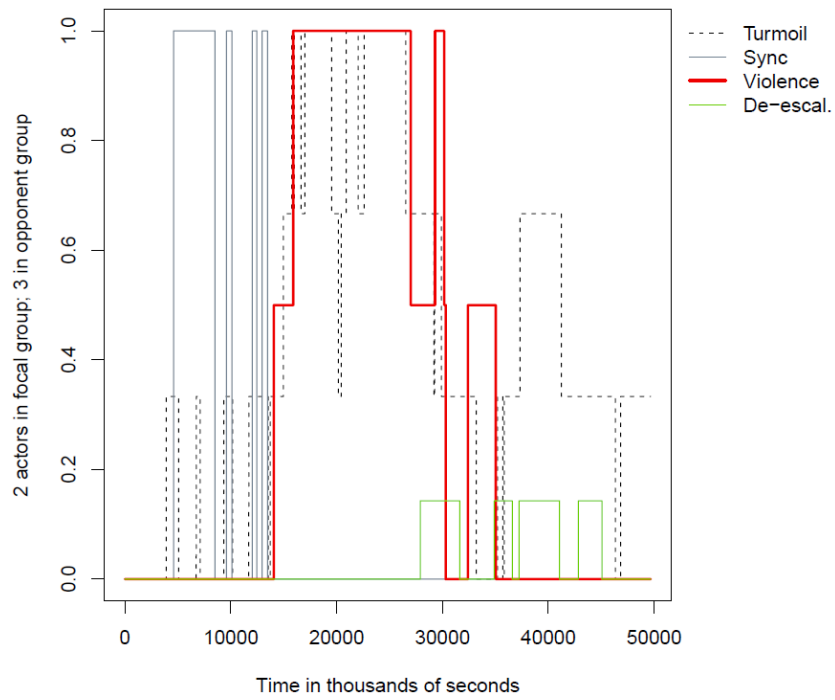


Figure 10: Graph of clip 26 with a burst of collective violence in a dyad.



Figure 11: Still taken from clip 86 at 0:59 seconds.



Figure 12: Still taken from clip 86 at 1:03 seconds.

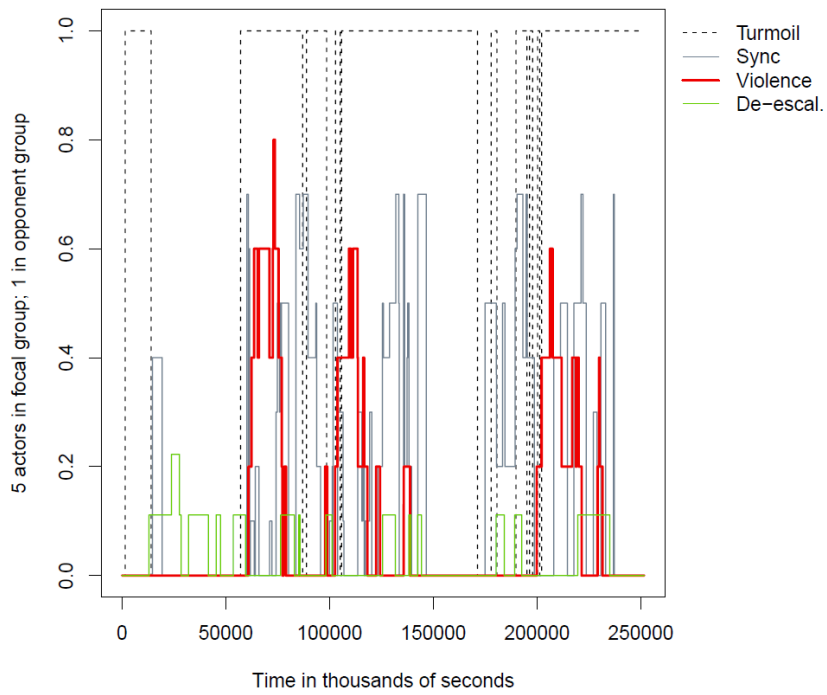


Figure 13: Graph of clip 86. Outbreaks of collective violence in a group of five. Because the time between the first and last participant's commencement of violence exceeds 2 seconds, these outbreaks are not classified as bursts.

## 10 Analysis of coded and plotted videos

We used graphs of coded videos in our analysis, illustrated in Fig. S14, where the opponent group in clip 67 is plotted. The horizontal axis is the timeline in thousands of seconds, the vertical axis is the proportion of group members involved (for turmoil and violence), and the proportion of intragroup ties involved out of the maximum possible number of ties (for synchrony of action). The first moment of collective violence, denoted by the downward arrow, involves two focal group members. There is, however, a short interruption of collective violent action. Therefore, we did not code this occurrence of collective violence as a burst. The time gap between the first participant and maximum participation in collective violence, denoted by the horizontal arrows, takes over 6 seconds.

In the figure, seven instances of turmoil occur (numbered 1-7) prior to the moment of maximum participation in violence: (1) a short interval that, after a brief interruption, continues for 4 seconds and involves 67% of the opponent group (2 members); (2) involves all three members of the opponent group and lasts nearly 1 second; (3) lasts less than 1 second and involves 33% of the opponent group; (4) turmoil continues, with an intermittent short dip, for over 1 second with 67% involvement; (5) a peak at 100% involvement that lasts less than 1 second; (6) a short drop to 67% involvement that takes approximately 1 second; (7) the last turmoil before maximal violence. We calculated the level of turmoil by multiplying the time length of each of these intervals by the number of actors involved.

Intervals of synchrony in Fig. S14 are indicated by A and B. A lasted 2.4 seconds and involved all ties in the group; B involved 67% of the ties for approximately 2 seconds prior to maximum participation in violence. Finally, the graph shows intervals of deescalatory action.

## 11 Overview of cases and descriptive statistics

Our dataset contains information about the behavior of 406 individuals in 42 violent incidents. The 59 groups and their key characteristics are listed in Table S1. After focal and opponent groups have been analyzed as listed, they flip roles with respect to cooperation and turmoil production in a second batch of the analysis, except when an opponent is solitary instead of a group.

	group	$n$	c.v.	$N_C$	lag	burst	$T$	Sync	$N_D$
1	1_beachfight_focal	3	1	2	0.00	1	0.97	19.39	1
2	3_asianeateries_focal	5	0	1		0	72.41	18.10	4

3	3.asianeateries_oppon.	2	0	1		0	93.37	16.20	1
4	6.rikshaddrivers_focal	6	1	4	1.93	1	7.24	5.33	2
5	7.baldies_focal	4	1	3	0.92	1	6.42	0.94	1
6	8.queensday_focal	14	1	6	1.95	1	45.81	303.42	8
7	9.gasstation_focal	2	0	1		0	14.49	16.30	1
8	10.redpickup_focal	3	1	3	0.93	1	9.34	78.75	0
9	26.insideeatery_focal	3	1	3	1.21	1	14.41	0.20	0
10	26.inseeatery_oppon.	2	1	2	1.77	1	7.49	5.32	0
11	27.dallasairport_focal	6	1	5	0.00	1	24.99	3.53	1
12	32.shovedbycar_focal	3	1	2	3.66	0	3.66	0.00	1
13	41.kababshop_focal	2	0	1		0	42.12	0.00	1
14	41.kababshop_oppon.	2	1	2	0.84	1	5.90	0.42	0
15	45.onbusystreet_focal	2	1	2	1.48	1	12.79	9.35	0
16	50.fitness_focal	2	1	2	3.08	0	4.62	1.54	0
17	52.blockingskaters_focal	2	0	1		0	20.44	10.72	1
18	52.blockingskaters_oppon.	4	0	1		0	45.56	17.36	3
19	53.famousonyoutube_focal	2	1	2	20.23	0	14.45	0.00	1
20	53.famousonyoutube_opp.	2	0	1		0	51.11	0.00	1
21	54.hammeronhead_focal	4	1	3	1.57	1	9.17	4.19	1
22	54.hammeronhead_oppon.	2	1	2	1.57	1	31.43	5.24	0
23	60.gangattack_focal	6	0	1		0	31.73	80.43	5
24	61.burgerking_focal	2	0	1		0	37.88	0.00	1
25	66.guyvsgang_focal	6	1	6	1.81	1	0.91	19.22	0
26	67.poolfight_focal	3	1	2	0.84	1	16.46	4.36	1
27	67.poolfight_oppon.	3	1	3	6.29	0	19.87	2.49	1
28	84.brokenwindow_focal	3	0	1		0	35.36	2.89	2
29	86.tables_focal	5	1	4	2.25	0	29.23	4.50	1
30	88.babypowder_focal	2	1	2	2.10	1	5.43	4.20	0
31	92.didntdoanything_focal	2	0	1		0	46.51	8.35	1
32	93.grouppkicking_focal	4	1	3	5.92	0	8.68	10.02	1
33	95.apologise_focal	9	1	2	1.51	0	26.42	76.30	7
34	95.apologise_oppon.	2	0	1		0	133.06	2.64	1
35	96.gangversusbat_focal	6	0	1		0	25.00	67.06	5
36	97.alleyfight_focal	4	0	1		0	61.14	26.32	4
37	97.alleyfight_oppon.	4	1	2	0.76	1	34.39	3.83	2
38	98.stopmick_focal	3	1	2	0.76	1	20.61	17.54	1
39	98.stopmick_oppon.	2	0	1		0	68.10	10.70	1
40	101.fightandrob_focal	6	1	4	2.97	0	22.19	21.45	2
41	101.fightandrob_oppon.	2	0	1		0	79.09	3.10	1
42	104.waiting_focal	4	1	4	0.73	1	13.83	0.36	0
43	104.waiting_oppon.	2	0	1		0	128.82	0.36	1
44	105.frenziedassault_focal	3	1	2	1.21	1	0.00	9.61	1
45	108.sidewalkbrawl_focal	2	0	1		0	268.40	44.73	1
46	108.sidewalkbrawl_oppon.	4	1	2	0.00	1	33.55	36.72	2
47	110.nietklaar_focal	5	1	3	14.45	0	36.13	12.04	1
48	121.eightballjacket_focal	4	1	3	2.66	0	8.64	1.08	1
49	124.leavehimalone_focal	3	1	3	4.86	0	13.36	0.00	0
50	124.leavehimalone_oppon.	2	1	2	0.00	1	9.09	0.00	0
51	128.throwingfood_focal	2	1	2	1.14	1	0.57	0.00	0

52	128_throwingfood_oppon.	2	1	2	2.28	0	6.83	0.00	0
53	129_awayfrommyfood_focal	5	1	2	3.06	0	14.22	4.09	3
54	129_awayfrommyfood_oppon.	6	0	1		0	65.37	30.00	5
55	133_homeboy_focal	2	1	2	2.68	0	0.54	1.07	0
56	134_down_focalgroup	4	1	2	0.89	1	23.12	45.27	2
57	134_down_oppon.	5	1	2	0.89	0	40.02	9.34	3
58	138_cometomyhouse_focal	3	0	0		0	34.02	36.51	3
59	145_knifefightcolombia_focal	2	0	1		0	17.04	20.16	1

Table S1: Overview of all groups and their sizes; occurrence of collective violence (c.v.); maximum participation in violence ( $N_C$ ); time lag between the first participant and maximum participation in collective violence; burst; levels of turmoil ( $T$ ) and of synchrony at first violence outbreak; number of unconditional defectors ( $N_D$ ). In group 8\_queensday, two focal group members disappeared from view already before the first moment of violence had started; out of the remaining 12, 6 participated in collective violence.

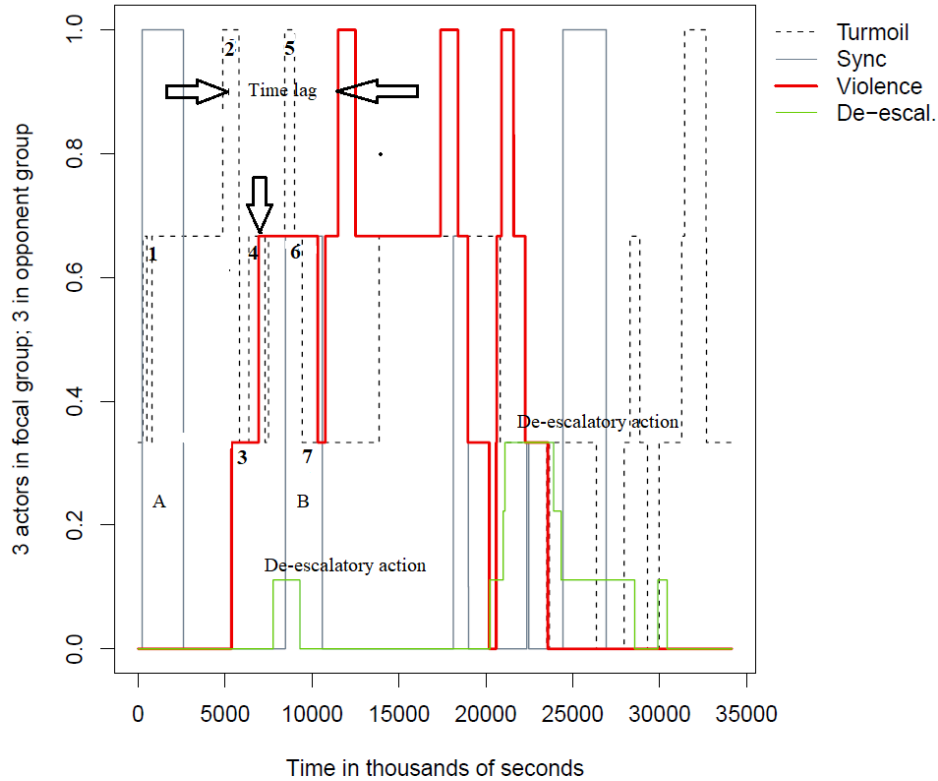


Figure 14: Graph of clip 67; opponent group. The timeline displays the start of collective violent action (downward arrow), instances of turmoil (1-7), synchrony (A,B), the time lag between the first and last group member joining the collective violence (horizontal arrows), and deescalatory action.

Table S2 provides mean values, percentages, standard deviations, and minimum and maximum values for the indicators used in the analysis.

## 12 Solving the Ising model

The Ising model can be solved computationally by the Metropolis algorithm (main text). Here, it is solved analytically by a mean field analysis, first for  $p = 0$  and then  $p > 0$ . Subsequently, deviations of the computational results from the mean field result are pointed out.

		mean or $n$ (%)	s.d.	min	max
1	Group size	3.58	2.09	2	14
2	Dyads	24 (40.7)		0	1
3	Triads	11 (18.6)		0	1
4	Groups $\geq 4$ members	24 (40.7)		0	1
5	Collective violence	38 (64.4)		0	1
6	Burst	23 (39)		0	1
7	Maximum participation in violence	.64	.28	0	1
8	Average time lag in bursts in sec. ( $n = 23$ )	1.06	.65	0	2.10
9	Average time lag per participant in non-bursts ( $n = 15$ )	5.12	5.29	0.89	20.23
10	Turmoil prior to max participation in violence ( $n = 38$ )	37 (97.4)		0	1
11	Level of turmoil prior to max part. in violence ( $n = 38$ )	15.34	12.21	0	45.81
12	Synchrony prior to max part. in violence ( $n = 38$ )	32 (84.2)		0	1
13	Level of synchrony prior to max part. in violence ( $n = 38$ )	18.98	50.95	0	303.42
14	Proportion unconditional defectors	.37	.28	0	1.0

Table 2: Descriptive statistics of indicators used in the analysis ( $\mathcal{N}=59$ ). Note: Levels of synchrony prior to maximum violence includes an outlier of 303.42. Without outlier, mean = 11.29; s.d. = 18.96; max = 78.75. We excluded this outlier in the calculations reported.

## 12.1 Mean field analysis

For the mean field analysis, we assess the level of cooperation,  $N_C/n$ , in terms of the order parameter,  $M = 1/n \sum_{i=1}^n S_i$ . Consequently,  $N_C/n = (M+D)/(C+D)$ . The mean field assumption can be stated as  $S_i = \bar{S}_i = M$ . For the moment, the proportion of unconditional defectors,  $p = 0$ ; see below when  $p > 0$ .

We start out with the Hamiltonian,  $H = -\sum_{i,j} w_{ij} S_i S_j$ . We use the mapping  $\{C, -D\} \rightarrow \{S_0 + \Delta, S_0 - \Delta\}$  with bias  $S_0 = (C - D)/2$  and offset  $\Delta = (C + D)/2$  to rewrite the Hamiltonian as

$$H = -\sum_{i,j} w_{ij} (S_0 + \hat{S}_i)(S_0 + \hat{S}_j), \quad (4)$$

with  $\hat{S}_i$  and  $\hat{S}_j \in \{-\Delta, \Delta\}$ , and taking into account the row-normalization of the adjacency matrix ( $\sum_j w_{ij} = 1$ ) [10].

To calculate the Boltzmann probabilities of a single spin (or an individual's probabilities to cooperate or defect), we define the pertaining Hamiltonian

$$H_i = - \sum_j w_{ij} (S_0 + \hat{S}_i) (S_0 + \hat{S}_j) \quad (5)$$

$$\begin{aligned} H_i &= - \sum_j w_{ij} (S_0 + \hat{S}_i) M \\ &= -(S_0 + \hat{S}_i) M \\ H_i^\pm &= -S_0 M \mp \Delta M. \end{aligned} \quad (6)$$

In the subsequent derivation, we use no Boltzmann constant (and no  $\beta$  either), just  $T$ . The average value of a spin,  $\bar{S}_i$ , according to the Boltzmann distribution, with  $P(S_i^-)$  standing for the probability that  $S_i$  is negative and  $P(S_i^+)$  that it is positive, is

$$\begin{aligned} \bar{S}_i &= S^- P(S_i^-) + S^+ P(S_i^+) \quad (7) \\ &= \frac{S^- e^{-H_i^-/T} + S^+ e^{-H_i^+/T}}{e^{-H_i^-/T} + e^{-H_i^+/T}} \\ &= \frac{S^- e^{-(-S_0 M + \Delta M)/T} + S^+ e^{-(-S_0 M - \Delta M)/T}}{e^{(-S_0 M + \Delta M)/T} + e^{(-S_0 M - \Delta M)/T}} \\ &= \frac{S^- e^{-\Delta M/T} + S^+ e^{\Delta M/T}}{e^{-\Delta M/T} + e^{\Delta M/T}} \\ &= \frac{(S_0 - \Delta) e^{-\Delta M/T} + (S_0 + \Delta) e^{\Delta M/T}}{e^{-\Delta M/T} + e^{\Delta M/T}} \\ &= S_0 \frac{e^{-\Delta M/T} + e^{\Delta M/T}}{e^{-\Delta M/T} + e^{\Delta M/T}} + \Delta \frac{-e^{-\Delta M/T} + e^{\Delta M/T}}{e^{-\Delta M/T} + e^{\Delta M/T}} \\ &= S_0 + \Delta \tanh(\Delta M/T). \end{aligned} \quad (8)$$

This result without unconditional defectors was inferred in an earlier study [10]. Here, we also deal with unconditional defectors in proportion  $p > 0$ . Accordingly, we define  $M_{cc}$  as the average spin value of the conditional cooperators and  $M_{ud}$  as the average spin value of the unconditional defectors. Note that  $M_{ud} = S^-$ . We assume that the unconditional defectors are homogeneously distributed across the network. Accordingly, the mean field equation becomes

$$S_i = p S^- + (1 - p) M_{cc}. \quad (9)$$

The Hamiltonian for a single conditional cooperator becomes

$$H_i^\pm = -(S_0 \pm \Delta) (p S^- + (1 - p) M_{cc}) \quad (10)$$

$$= -S_0 p S^- \mp \Delta p S^- - S_0 (1 - p) M_{cc} \mp \Delta (1 - p) M_{cc}. \quad (11)$$

In the derivation of Eq. 8, all terms that did not contain  $\mp\Delta$  canceled each other out. For clarity, we remove these terms from Eq. 11, which results in

$$H_i^\pm = \mp\Delta(pS^- + (1-p)M_{cc}). \quad (12)$$

The mean field analysis for conditional cooperators  $i$  is

$$\begin{aligned} \bar{S}_i &= S^- P(S_i^-) + S^+ P(S_i^+) \\ &= \frac{S^- e^{-\Delta(pS^- + (1-p)M_{cc})/T} + S^+ e^{\Delta(pS^- + (1-p)M_{cc})/T}}{e^{-\Delta(pS^- + (1-p)M_{cc})/T} + e^{\Delta(pS^- + (1-p)M_{cc})/T}} \\ &= S_0 + \Delta \frac{-e^{-\Delta(pS^- + (1-p)M_{cc})/T} + e^{\Delta(pS^- + (1-p)M_{cc})/T}}{e^{-\Delta(pS^- + (1-p)M_{cc})/T} + e^{\Delta(pS^- + (1-p)M_{cc})/T}} \\ &= S_0 + \Delta \tanh(\Delta(pS^- + (1-p)M_{cc})/T) = M_{cc}. \end{aligned} \quad (13)$$

Using Eq. 9, we can express the self-consistency equation of  $M_{cc}$  in  $M$ ,

$$\begin{aligned} M &= pS^- + (1-p)(S_0 + \Delta \tanh(\Delta(pS^- + (1-p)M_{cc})/T)) \\ &= pS^- + (1-p)(S_0 + \Delta \tanh(\Delta M/T)) \\ &= S_0 - p\Delta + (1-p)\Delta \tanh(\Delta M/T). \end{aligned} \quad (14)$$

## 12.2 Critical proportion of unconditional defectors

Depending on  $T$ , the self-consistency equation has one unstable and two stable ferromagnetic solutions, or one stable paramagnetic solution. At a critical  $T$ , the system transitions between these two states. When the system is paramagnetic,

$$\frac{\partial}{\partial M}(S_0 - p\Delta + (1-p)\Delta \tanh(\Delta M/T)) < 1$$

at the solution of  $M$ . When the system is ferromagnetic,

$$\frac{\partial}{\partial M}(S_0 - p\Delta + (1-p)\Delta \tanh(\Delta M/T)) > 1$$

at the unstable solution of  $M$ . We can identify a critical  $T$  when

$$\frac{\partial}{\partial M}(S_0 - p\Delta + (1-p)\Delta \tanh(\Delta M/T)) = 1, \quad (15)$$

hence,

$$\begin{aligned}
\frac{1}{\cosh^2(\Delta M/T)} \Delta^2(1-p)/T &= 1 \\
\cosh(\Delta M/T) &= \sqrt{\Delta^2(1-p)/T} \\
\Delta M/T &= \pm \operatorname{arcosh}(\sqrt{\Delta^2(1-p)/T}) \\
\frac{M}{\Delta} &= \frac{\pm \operatorname{arcosh}(\sqrt{\Delta^2(1-p)/T})}{\Delta^2/T}. \quad (16)
\end{aligned}$$

We can substitute this expression (16) in the self-consistency equation (14)

$$\begin{aligned}
\frac{\pm \operatorname{arcosh}(\sqrt{\Delta^2(1-p)/T})}{\Delta/T} &= S_0 - p\Delta + (1-p)\Delta \tanh(\pm \operatorname{arcosh}(\sqrt{\Delta^2(1-p)/T})) \\
\frac{\pm \operatorname{arcosh}(\sqrt{\Delta^2(1-p)/T})}{\Delta^2/T} &= \frac{S_0}{\Delta} - p \pm (1-p) \tanh(\operatorname{arcosh}(\sqrt{\Delta^2(1-p)/T})) \\
&= \frac{S_0}{\Delta} - p \pm (1-p) \sqrt{1 - \frac{1}{\Delta^2(1-p)/T}}. \quad (17)
\end{aligned}$$

Discarding the equation that has no real numerical solutions leaves

$$-\frac{\operatorname{arcosh}(\sqrt{\Delta^2(1-p)/T})}{\Delta^2/T} + (1-p) \sqrt{1 - \frac{1}{\Delta^2(1-p)/T}} = \frac{S_0}{\Delta} - p. \quad (18)$$

Solutions of this equation become complex if  $p > \frac{S_0}{\Delta}$ , hence  $p \leq \frac{S_0}{\Delta}$ . Graphical illustrations are in Fig. S15. The choice of  $C = 1$  and  $D = 1/2$  implies that there is no (burst of) cooperation if  $p > 1/3$ .

### 12.3 Solving the Ising model computationally

The Ising model was solved computationally, in Fortran for speed and in R for comfort. Surprisingly,  $p_c$  of simulated, fully connected networks is very close to the mean field calculation of  $p_c$ , even in very small networks. Given  $C = 1$  and  $D = 1/2$ , there is no burst if  $p_c > 0.34$ . The critical threshold is nearly density independent: if in (sufficiently large) simulated networks, density is decreased by two orders of magnitude,  $p_c$  increases from  $\approx 0.34$  to  $\approx 0.35$ . The degree distribution has no effect on  $p_c$ .

In simulations,  $p_c$  is less precise in smaller networks (Table S3) and the prediction for the triad is empirically false, whereas the mean field is correct: one unconditional defector does not prevent cooperation of the other two. Also one empirical group of six with two unconditional defectors had a burst, which did not happen in the simulations.

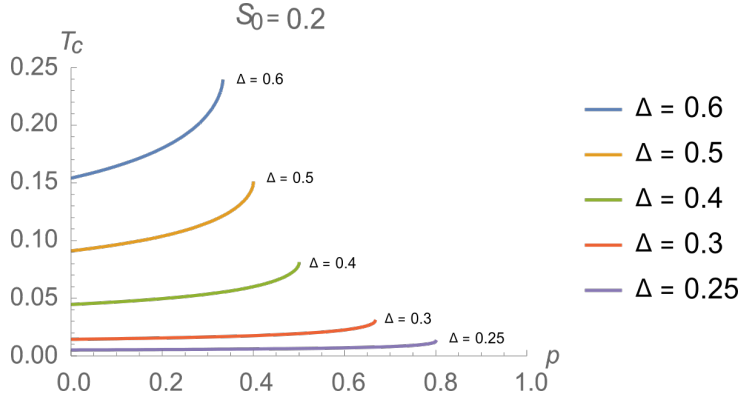


Figure 15: Given  $S_0 = 0.2$ , the critical level of agitation,  $T_c$ , is plotted as a function of the proportion of unconditional defectors,  $p$ , for various levels of  $\Delta$ . The critical level,  $p_c$ , is reached at the right-hand end of the lines.

$n$	$N_D$	$\approx N_C$	burst
2	1	0	0
3	1	1	0
4	1	2	1
5	1	3-4	1
6	1	4-5	1
5	2	1	0
6	2	2	0
7	2	4	1
8	2	4-5	1
9	2	6	1
9	3	3	0

Table 3: Simulations just below (burst = 1) and above (burst = 0) the critical threshold of unconditional defectors ( $N_D$ ) in small groups (size  $n$ ). The numbers of cooperators ( $N_C$ ) fluctuate across simulation runs and are approximate. Note: For groups with  $n = 7$  and  $N_D = 2$ , simulations in Fortran yield  $N_C \approx 4$  whereas in  $R$ ,  $N_C \approx 3$ .

## Authors' contributions

JB made the asymmetric Ising model, and wrote the software and the paper. DW collected, interpreted, and analyzed the data. BM did the mean field analysis. JB and DW wrote the Supplementary Material.

## References

- [1] Christoph Adami and Arend Hintze. Thermodynamics of evolutionary games. *Physical Review E*, 97:062136, 2018.
- [2] Luciano Andreozzi, Matteo Ploner, and Ali Seyhun Saral. The stability of conditional cooperation: beliefs alone cannot explain the decline of cooperation in social dilemmas. *Scientific Reports*, 10:1–10, 2020.
- [3] Alex Arenas, Albert Díaz-Guilera, and Conrad J. Pérez-Vicente. Synchronization reveals topological scales in complex networks. *Physical Review Letters*, 96:114102, 2006.
- [4] Daniel Bar-Tal. The necessity of observing real life situations. *European Journal of Social Psychology*, 34:677–701, 2004.
- [5] Alain Barrat, Marc Barthélemy, and Alessandro Vespignani. *Dynamical Processes on Complex Networks*. Cambridge University Press, New York, 2008.
- [6] Elwood M Beck and Stewart E. Tolnay. The killing fields of the Deep South: The market for cotton and the lynching of blacks, 1882-1930. *American Sociological Review*, 55:526–539, 1990.
- [7] Peter Blau. *Exchange and Power in Social Life*. Transaction Publishers, New Brunswick, 2nd 1986 edition, 1964.
- [8] Jeroen Bruggeman. *A Sociology of Humankind*. Routledge, New York, 2024.
- [9] Jeroen Bruggeman and Rudolf Sprik. Cooperation for public goods under uncertainty. *Lecture Notes in Computer Science*, 12140:243–251, 2020.
- [10] Jeroen Bruggeman, Rudolf Sprik, and Rick Quax. Spontaneous cooperation for public goods. *Journal of Mathematical Sociology*, 45:183–191, 2021.
- [11] Maxwell N. Burton-Chellew and Stuart A. West. Payoff-based learning best explains the rate of decline in cooperation across 237 public-goods games. *Nature Human Behaviour*, 5:1330–1338, 2021.
- [12] Claudio Castellano, Santo Fortunato, and Vittorio Loreto. Statistical physics of social dynamics. *Reviews of Modern Physics*, 81:591, 2009.
- [13] Ananish Chaudhuri. Sustaining cooperation in laboratory public goods experiments. *Experimental Economics*, 14:47–83, 2011.
- [14] Robert B. Cialdini and Noah J. Goldstein. Social influence: Compliance and conformity. *Annual Review of Psychology*, 55:591–621, 2004.
- [15] Randall Collins. *Violence: A Micro-Sociological Theory*. Princeton University Press, Princeton, NJ, 2008.
- [16] Bryan C. Daniels, David C. Krakauer, and Jessica C. Flack. Control of finite critical behaviour in a small-scale social system. *Nature Communications*, 8:14301, 2017.
- [17] D. Dion and R. Axelrod. The further evolution of cooperation. *Science*, 242:1385–1390, 1988.
- [18] Emile Durkheim. *Les formes élémentaires de la vie religieuse*. Presses Universitaires de France, Paris, 1912.

- [19] Ernst Fehr and Urs Fischbacher. The nature of human altruism. *Nature*, 425:785, 2003.
- [20] Ronald Fischer, Rohan Callander, Paul Reddish, and Joseph Bulbulia. How do rituals affect cooperation? *Human Nature*, 24:115–125, 2013.
- [21] Noah E. Friedkin and Eugene C. Johnsen. *Social Influence Network Theory*. Cambridge University Press, Cambridge, MA, 2011.
- [22] Serge Galam and Serge Moscovici. Towards a theory of collective phenomena. *European Journal of Social Psychology*, 21(1):49–74, 1991.
- [23] Luke Glowacki and Rose McDermott. Key individuals catalyse intergroup violence. *Philosophical Transactions of the Royal Society B*, 377:20210141, 2022.
- [24] Sandra González-Bailón, Javier Borge-Holthoefer, Alejandro Rivero, and Yamir Moreno. The dynamics of protest recruitment through an online network. *Scientific Reports*, 1:1–7, 2011.
- [25] Mark Granovetter. Threshold models of collective behavior. *American Journal of Sociology*, 83:1420–1443, 1978.
- [26] Garrett Hardin. The tragedy of the commons. *Science*, 162:1243–1248, 1968.
- [27] Brandon Ives and Jacob S. Lewis. From rallies to riots. *Journal of Conflict Resolution*, 64:958–986, 2020.
- [28] Neil F. Johnson, M. Zheng, Yulia Vorobyeva, Andrew Gabriel, Hong Qi, Nicolás Velásquez, Pedro Manrique, Daniela Johnson, E. Restrepo, Chaoming Song, et al. New online ecology of adversarial aggregates: Isis and beyond. *Science*, 352:1459–1463, 2016.
- [29] Frank L. Jones. Simulation models of group segregation. *The Australian and New Zealand Journal of Sociology*, 21:431–444, 1985.
- [30] Nikki Jones and Geoffrey Raymond. The camera rolls: Using third-party video in field research. *Annals of the American Academy of Political and Social Science*, 642:109–123, 2012.
- [31] Sigismund Kobe. Ernst Ising 1900-1998. *Brazilian Journal of Physics*, 30:649–654, 2000.
- [32] Mark Levine, Paul J. Taylor, and Rachel Best. Third parties, violence, and conflict resolution. *Psychological Science*, 22:406–412, 2011.
- [33] Lasse Suonperä Liebst, Richard Philpot, Wim Bernasco, Kasper Lykke Dausel, Peter Ejbye-Ernst, Mathias Holst Nicolaisen, and Marie Rosenkrantz Lindegaard. Social relations and presence of others predict bystander intervention. *Aggressive Behavior*, 45:598–609, 2019.
- [34] Paul Luff and Christian Heath. Some technical challenges of video analysis. *Qualitative Research*, 12:255–279, 2012.
- [35] Gerald Marwell and Pamela Oliver. *The Critical Mass in Collective Action*. Cambridge University Press, Cambridge, MA, 1993.
- [36] Omar Shahabudin McDoom. Who killed in Rwanda’s genocide? *Journal of Peace Research*, 50:453–467, 2013.

- [37] William H. McNeill. *Keeping Together in Time: Dance and Drill in Human History*. Harvard University Press, Cambridge, MA, 1995.
- [38] E-J Milne, Claudia Mitchell, and Naydene de Lange. *Handbook of Participatory Video*. AltaMira Press, Walnut Creek, CA, 2012.
- [39] T.J.H. Morgan, L.E. Rendell, Micael Ehn, W. Hoppitt, and K.N. Laland. The evolutionary basis of human social learning. *Proceedings of the Royal Society of London B*, 279:653–662, 2012.
- [40] Anne Nassauer. *Situational Breakdowns: Understanding Protest Violence and other Surprising Outcomes*. Oxford University Press, Oxford, 2019.
- [41] Martin A. Nowak and Karl Sigmund. Evolution of indirect reciprocity. *Nature*, 437:1291–1298, 2005.
- [42] Mancur Olson. *The Logic of Collective Action*. Harvard University Press, Harvard, 1965.
- [43] Elinor Ostrom. A general framework for analyzing sustainability of social-ecological systems. *Science*, 325:419–422, 2009.
- [44] Giorgio Parisi. Spin glasses and fragile glasses: Statics, dynamics, and complexity. *Proceedings of the National Academy of Sciences*, 103:7948–7955, 2006.
- [45] Matjaž Perc, Jillian J. Jordan, David G. Rand, Zhen Wang, Stefano Boccaletti, and Attila Szolnoki. Statistical physics of human cooperation. *Physics Reports*, 687:1–51, 2017.
- [46] Scott Phillips and Mark Cooney. Aiding peace, abetting violence: Third parties and the management of conflict. *American Sociological Review*, 70:334–354, 2005.
- [47] Richard Philpot, Lasse Suonperä Liebst, Mark Levine, Wim Bernasco, and Marie Rosenkrantz Lindegaard. Would I be helped? Cross-national CCTV footage shows that intervention is the norm in public conflicts. *American Psychologist*, 75:66–75, 2020.
- [48] Devesh Rustagi, Stefanie Engel, and Michael Kosfeld. Conditional cooperation and costly monitoring explain success in forest commons management. *Science*, 330:961–965, 2010.
- [49] Rim Saab, Russell Spears, Nicole Tausch, and Julia Sasse. Predicting aggressive collective action based on the efficacy of peaceful and aggressive actions. *European Journal of Social Psychology*, 46:529–543, 2016.
- [50] Shubhayan Sarkar and Colin Benjamin. Triggers for cooperative behavior in the thermodynamic limit: A case study in public goods game. *Chaos*, 29:053131, 2019.
- [51] Hirokazu Shirado and Nicholas A. Christakis. Locally noisy autonomous agents improve global human coordination in network experiments. *Nature*, 545:370–374, 2017.
- [52] Georg Simmel. *Soziologie*. Duncker and Humblot, Berlin, 1908.
- [53] Theda Skocpol. *States and Social Revolutions: A Comparative Analysis of France, Russia and China*. Cambridge University Press, Cambridge, UK, 1979.
- [54] Dietrich Stauffer and Sorin Solomon. Ising, Schelling and self-organising segregation. *European Physical Journal B*, 57:473–479, 2007.

- [55] Daniel L. Stein and Charles M. Newman. *Spin Glasses and Complexity*. Princeton University Press, Princeton, NJ, 2013.
- [56] William B. Swann, Jolanda Jetten, Ángel Gómez, Harvey Whitehouse, and Bastian Brock. When group membership gets personal: A theory of identity fusion. *Psychological Review*, 119:441–456, 2012.
- [57] Ulf Toelch and Raymond J. Dolan. Informational and normative influences in conformity from a neurocomputational perspective. *Trends in Cognitive Sciences*, 19:579–589, 2015.
- [58] Zeynep Tufekci. *Twitter and Tear Gas*. Yale University Press, New Haven, 2017.
- [59] Pieter Van den Berg and Tom Wenseleers. Uncertainty about social interactions leads to the evolution of social heuristics. *Nature Communications*, 9:2151, 2018.
- [60] J.C. Walter and G.T. Barkema. An introduction to Monte Carlo methods. *Physica A*, 418:78–87, 2015.
- [61] Duncan J. Watts. A simple model of global cascades on random networks. *Proceedings of the National Academy of Sciences*, 99:497–502, 2002.
- [62] Don Weenink. Frenzied attacks: A micro-sociological analysis of the emotional dynamics of extreme youth violence. *British Journal of Sociology*, 65:411–433, 2014.
- [63] Don Weenink, Raheel Dhattiwala, and David van der Duin. Circles of peace: A video analysis of situational group formation and collective third-party intervention in violent incidents. *British Journal of Criminology*, 62:18–36, 2022.
- [64] Wolfgang Weidlich. The statistical description of polarization phenomena in society. *British Journal of Mathematical and Statistical Psychology*, 24:251–266, 1971.
- [65] Jia-Jia Wu, Cong Li, Bo-Yu Zhang, Ross Cressman, and Yi Tao. The role of institutional incentives and the exemplar in promoting cooperation. *Scientific Reports*, 4:6421, 2014.